# AIRBORNE LIDAR INVESTIGATIONS OF THE AEROSOL POLLUTION OVER THE BAYKAL INTEGRATED PULP-AND-PAPER MILL

**G.P. Kokhanenko, I.E. Penner, and V.S. Shamanaev**

*Institute of Atmospheric Optics,*
*Siberian Branch of the Russian Academy of Sciences, Tomsk*
*Received January 26, 1996*

*Airborne lidar sensing of the aerosol pollution over the Integrated Pulp-and-Paper Mill (IPPM) located in the hollow of Lake Baykal has been carried out. Horizontal and vertical views of the extinction coefficients of radiation with a wavelength of* 532 nm *have been mapped. In the region of Integrated Pulp-and-Paper Mill the atmospheric column* 1.5 km *high with an area of* 1 $m^2$ *has been found to contain* 60–100 mg *of dust. Above the water the total content of pollutants has been found to decrease by an order of magnitude for IPPM from the windward side.*

Airborne lidar monitoring of the anthropogenic aerosol in industrial regions already has its own history[1,2] and has demonstrated its efficiency. The high expense of aircraft used as a lidar platform pays out because of a short time taken for observation of a large volume of the atmosphere over an enormous territory including the vertical atmospheric structure from the lidar to the underlying surface. In addition, application of an instrumentation complex extends the capabilities of data interpretation. It is especially important for an analysis of industrial emissions having complex composition.

The airborne experiments[3] have demonstrated that the atmosphere makes unexpectedly large contribution to the pollution of Lake Baykal waters. This stimulated our active interest to such an atmospheric pollutant as the Baykal Integrated Pulp-and-Paper Mill (IPPM).

In the experiment described in the present paper the lidar configuration[1] was changed: two receiving telescopes were used with one laser. The receiver of the Makrel'–2M lidar 0.2 m in diameter was used in the atmospheric channel without polarization analysis. Signals were picked up not only from the anode, but also from two intermediate (eighth and tenth) dynodes of the FEU–84–3 photomultiplier. These signals were recorded simultaneously by a multichannel analog-to-digital converter. A special technique for the lidar calibration in this regime of operation was devised to join the signals from different channels of the ADC on the same scale. This enabled us to extend the dynamic range of signal recording and to widen the linear part of the dynamic range of lidar operation without abrupt change of the sensitivity of a receiving system. Laser pulses were transmitted at a frequency of 5 Hz.

In the channel of sensing of the Lake Baykal water, we used one of the receiving telescopes of the Svetozar–3 lidar[4] 0.1 m in diameter and high-speed FEU–144 photomultipliers for polarization measurements. However, problems of hydrooptical sensing are beyond the scope of the present paper.

Inversion of lidar signals into profiles of the aerosol scattering coefficient was performed by the quadrature integration algorithm[5] with a reference point adjacent to the lidar. It is well known that the boundary conditions assigned at the origin of a sounding path essentially decrease the error of inversion of the lidar sensing equation. To measure the initial value of the scattering coefficient, the aircraft-laboratory was equipped with a nephelometer.[6]

The atmosphere above the IPPM was sounded from onboard the aircraft that flew around the traffic circuit above the shore and water area of Lake Baykal on June 15, 1995. Flights were conducted at altitudes of 1600, 1000, and 400 m above the water surface during 1.5 h.

The flight chart is shown in Fig. 1. In this figure, the dashed line shows the shore and black bars indicate positions of main smoke stacks. The directions of propagation of smoke plumes from the most intense sources of pollution over the measurement period are indicated with arrows. The aircraft approached from the sea (from the water surface of Lake Baykal), crossed the cape with the IPPM, and went again to the sea along a closed line. Small arrows with the numbers adjacent to them indicate the points of the flight lines for which the vertical profiles of the aerosol extinction coefficients will be given further (see Figs. 4*a* and *b* below).

0235-6880/96/06 484-05 $02.00 

The panoramic view of the vertical profile of the extinction coefficient $\varepsilon(h)$, measured when the aircraft flew at an altitude of 1000 m, is shown in Fig. 2 as gradations in gray color. The flight time is plotted on the abscissa; 1 min corresponds to approximately 5 km pass. The barometer altitude was kept constant by the aircraft and therefore transition from the water surface to the dry land noticeably rising above the lake level is clearly seen. Figure 3 shows the panoramic view of the vertical profile of $\varepsilon$ measured when the aircraft flew at an altitude of 1600 m. At the left of Fig. 3 the vertical profiles of the temperature measured during the aircraft takeoff in Irkutsk (at 11:10, L.T.) and in the region of measurements (at 12:30, L.T.) are shown. The air temperature above the lake could not be measured at altitudes below 400 m because of the flight conditions. Instantaneous profiles of the extinction coefficients for these panoramic views (at points 1–8 of the flight route, see Fig. 1) are shown in Figs. 4*a* and *b* with the same numbers.

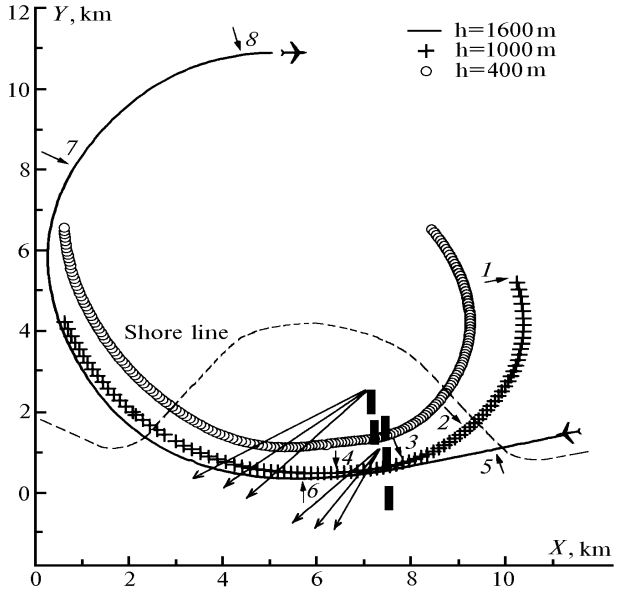


*FIG. 1. Flight chart of pollution sensing. The water surface is at the top and dry land is at the bottom, shore line is shown with the dashed curve. Routes of flight at altitudes of* 1600, 1000, *and* 400 m *are mapped out. Black bars indicate the main smoke stacks of the IPPM. Small arrows with the adjacent numbers indicate the points of sensing. Large arrows indicate prevailing wind directions.*

The aerosol formation was not a narrow extended plume. The stacks together represent an aerosol generator producing an asymmetric pancake formation. Its top was formed by the temperature inversion extended to 600 m. The boundary of the most dense layer was within the 400–450 m altitude range having the largest temperature gradient. In the shore line from the windward side (curves *2* and *5* in Fig. 4 and after ~1 min flight in Fig. 2) puffs of smoke can be seen above 400 m, with the aerosol particle density being higher than that in the main layer. A weak 600-m layer is most clearly pronounced here. The maximum aerosol density was recorded when the aircraft flew through the most intense smoke plume (curves *4* and *6*). In this case, the extinction coefficient reached 1 $km^{-1}$. It should be noted that the maximum extinction coefficient reached 2.2 $km^{-1}$ when the aircraft flew at an altitude of 400 m in the immediate vicinity of the source of pollutants.

The density of the smoke layer gradually decreased with distance from the shore and was minimum at point *8*. Here, the background profile of $\varepsilon(h)$ was nearly constant (within the limits of experimental error) at altitudes above 400 m. The analogous profile was obtained from the windward side of the shore (curve *1* in Fig. 4*a*).

Recall that the initial values of the extinction coefficient were measured by the nephelometer at the beginning of each flight circuit and then averaged over a few seconds. The background values of $\varepsilon$ varied smoothly in the range 0.015–0.024 $km^{-1}$ at an altitude of 1600 m (for 23 minutes of flight) and in the range 0.028–0.055 $km^{-1}$ for 25 minutes of flight at an altitude of 1000 m, while the vertical variations of $\varepsilon(h)$ at altitudes above 600 m, recorded during the aircraft descent, were much lower. In accordance with this, profiles 1 and 8, recorded from the windward side of the shore, indicate that at great altitudes the extinction coefficient changed twice but remained nearly constant ($\varepsilon \approx 0.025$ $km^{-1}$) near the water surface.

Our measurements lasted a short period. However, the structure of pollution described above existed for a long time. Therefore, it was interesting to evaluate the integrated content of aerosols in the atmospheric column above a unit surface area. This parameter can be tentatively called total equivalent aerosol amount $m_e = \int m(h)\mathrm{d}h = \mu \int \varepsilon(h)\mathrm{d}h$, where $m$ is the aerosol mass concentration. The parameter $m_e$ and the optical thickness $\tau$ (to the natural base) measured with the lidar are related by the expression $m_e = \mu\tau$, where $\mu$ is the coefficient of regression between the mass concentration $m$ and the extinction coefficient $\varepsilon$. According to Ref. 5, $\mu = (0.52 \pm 0.34)$ mg·km/$m^3$ for a wide class of industrial pollutants.

Figure 5 shows the horizontal profile of instantaneous values of the optical thickness corresponding to the panoramic view of Fig. 3. The total equivalent aerosol amount was varied from 15 to 60 mg/$m^2$. The minimum value of $m_e$ measured well offshore was 10 mg/$m^2$. It is natural to assume that the maximum values of $m_e$ will be slightly higher in the vicinity of smoke stacks.

As a whole, summarizing the results of our experiments, we can emphasize the following main points:

1. The aerosol cap above the IPPM is formed typically as a result of joint effect of the temperature inversion and prevailing wind.

2. The background aerosol extinction coefficient above the water surface of Lake Baykal is approximately constant at altitudes up to 1.5 km.

3. The measured value of the total equivalent aerosol amount in the atmospheric column of unit area is 60–100 mg/m$^2$ in most polluted regions above the IPPM and decreases by an order of magnitude at a distance of 10 km from the shore.

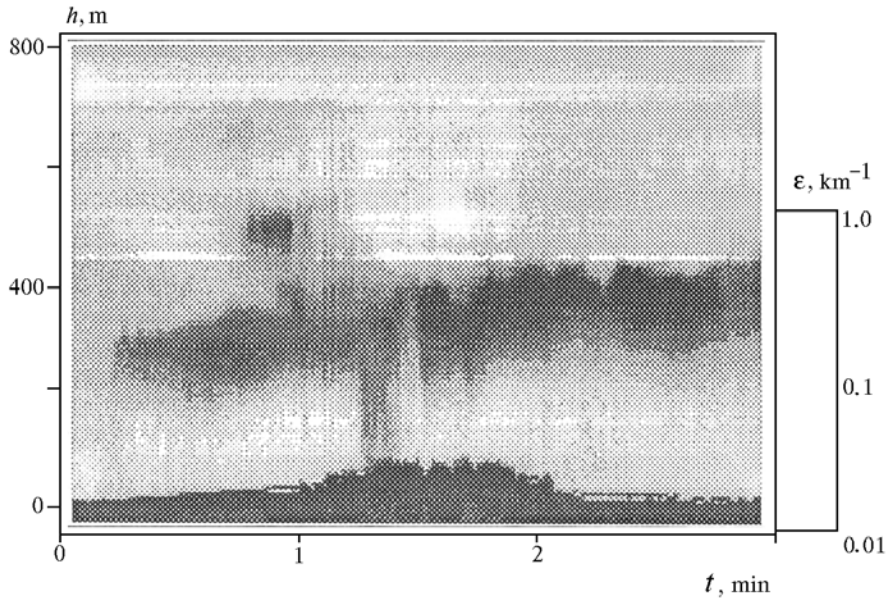


*FIG. 2. Panoramic view of the extinction coefficient profile* ε(*h*) *measured in flight at an altitude of* 1000 m.

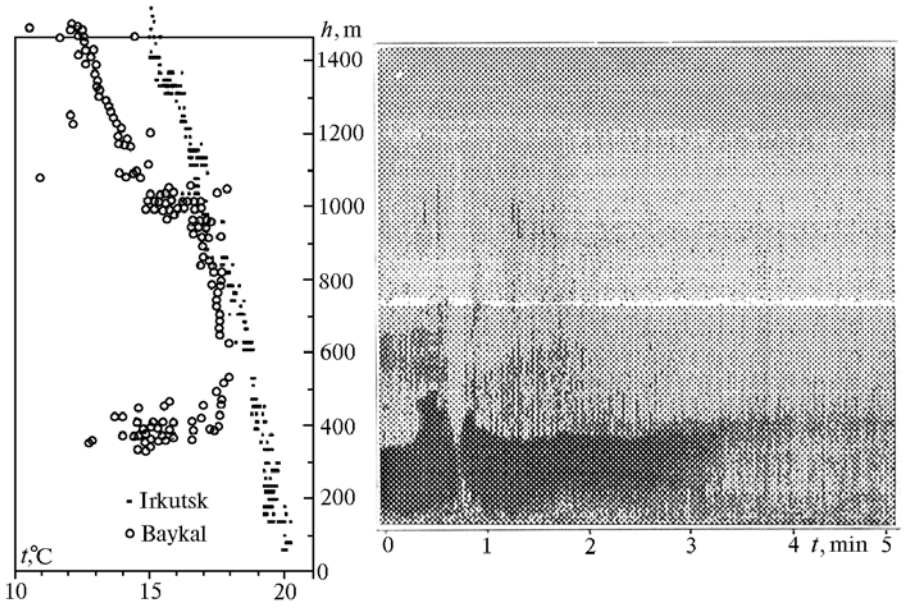


*FIG. 3. Panoramic view of the profile of* ε(*h*) *measured in flight at an altitude of* 1600 m. *At the left of the figure the profiles of the temperature measured during the aircraft takeoff in Irkutsk and above the IPPM are shown in the frame.*

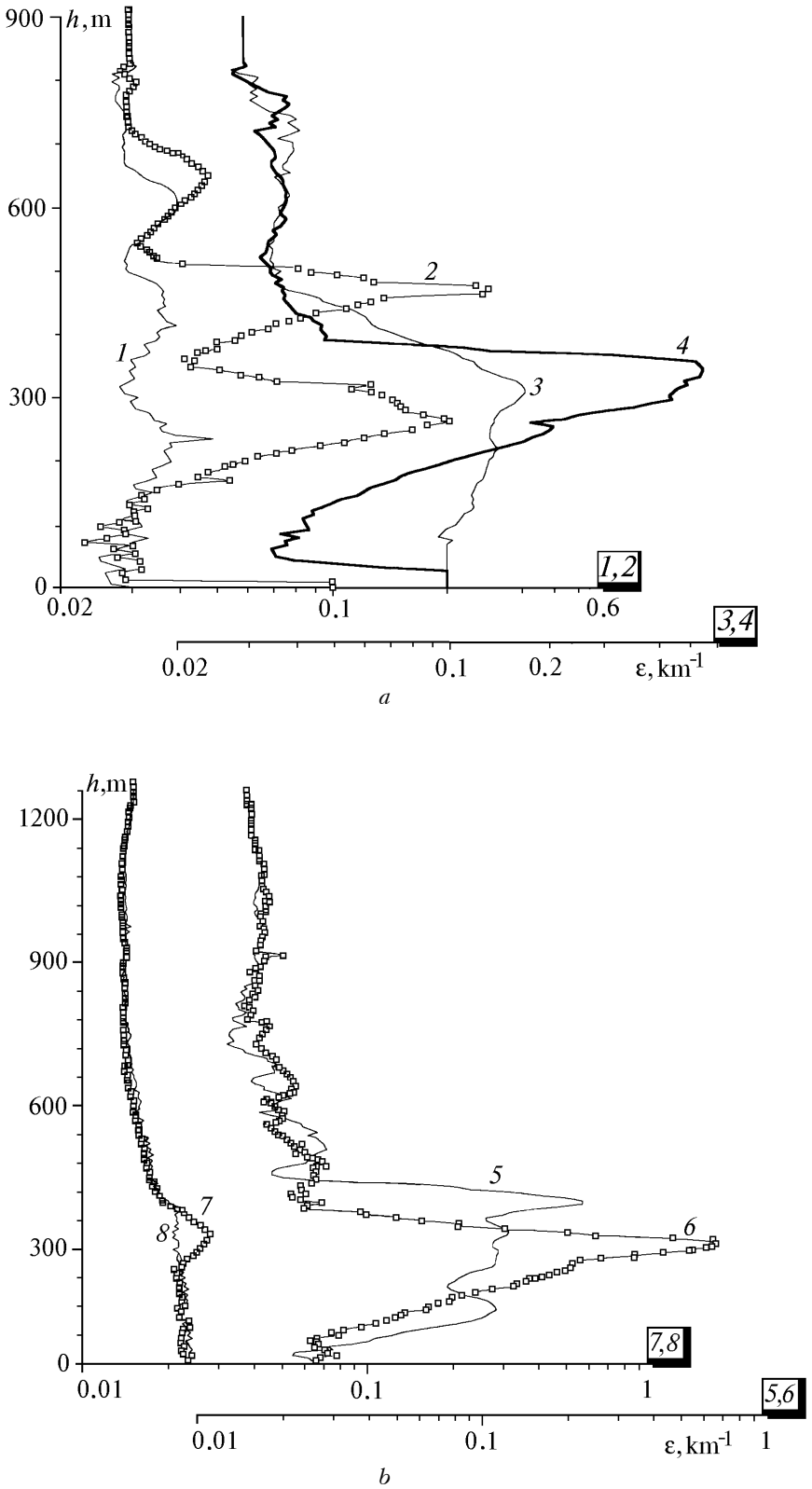


*FIG. 4. Vertical profiles of the extinction coefficients measured in flight at altitudes* 1000 *(a) and* 1600 m *(b). The numbers adjacent to curves correspond to the numbers of points on the flight lines of Fig. 1.*

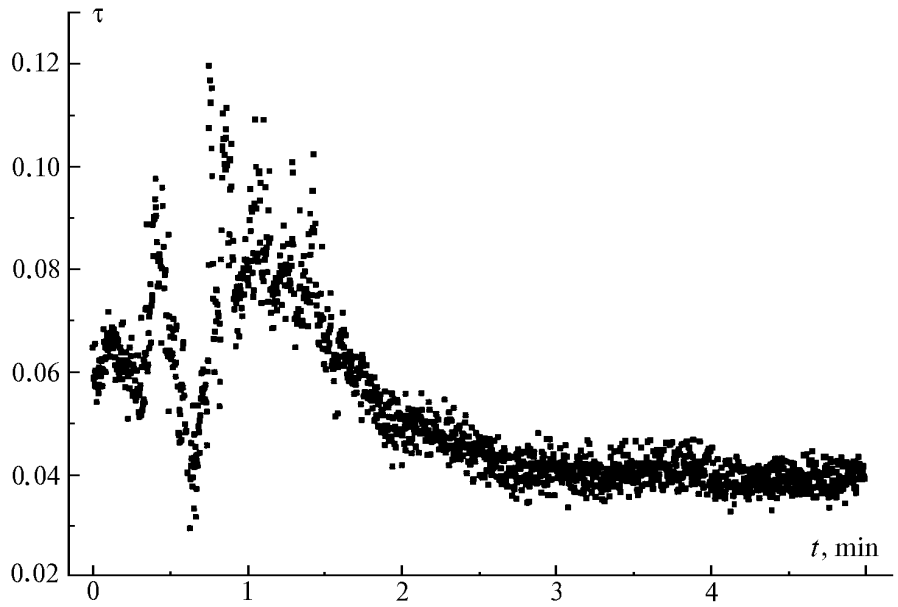


*FIG. 5. Horizontal profile of the optical thickness* τ *corresponding to the panoramic view of Fig. 3.*

## ACKNOWLEDGMENT

This work was supported in part by Russian Foundation of Fundamental Researches Grant No. 95–05–16562, International Scientific Foundation Grant No. NY2000, and International Scientific Foundation and Russian Federation Government Grant No. NY2300.

## REFERENCES

1. B.D. Belan, V.V. Burkov, M.V. Panchenko, et al., Atmos. Oceanic Opt. **5**, No. 2, 121–125 (1992).
2. I.E. Penner and V.S. Shamanaev, Atmos. Oceanic Opt. **7**, No. 3, 178–181 (1994).
3. V.E. Zuev, V.V. Antonovich, B.D. Belan, et al., Dokl. Akad. Nauk **325**, No. 6, 1146–1150 (1992).
4. V.S. Shamanaev and A.I. Abramochkin, "*Airborne polarization lidar Svetozar-3*,B VINITI, No. 6222–85 Dep., Moscow, August 21, 1985.
5. M.V. Kabanov, ed., *Laser Sensing of the Industrial Aerosols* (Nauka, Novosibirsk, 1986), 188 pp.
6. M.V. Panchenko, S.A. Terpugova, A.G. Tumakov, et al., Atmos. Oceanic Opt. **7**, No. 8, 546–551 (1994).